Advances in Aircraft and Spacecraft Science, *Vol. 5, No. 4 (2018) 499-513*
DOI: https://doi.org/10.12989/aas.2018.5.4.499

Monitoring the water absorption in GFRE pipes via an electrical capacitance sensors

Wael A. Altabey *[1,2,3] and Mohammad Noori[1,4]

[1]*International Institute for Urban Systems Engineering, Southeast University, Nanjing, Jiangsu, China*
[2]*Nanjing Zhixing Information Technology Co., Ltd., Andemen Street, Nanjing, Jiangsu, China*
[3]*Department of Mechanical Engineering, Faculty of Engineering, Alexandria University, Alexandria, Egypt*
[4]*Department of Mechanical Engineering, California Polytechnic State University, San Luis Obispo, CA, USA*

(Received July 20, 2017, Revised October 09, 2017, Accepted May 24, 2018)

Abstract. One of the major problems in glass fiber reinforced epoxy (GFRE) composite pipes is the durability under water absorption. This condition is generally recognized to cause degradations in strength and mechanical properties. Therefore, there is a need for an intelligent system for detecting the absorption rate and computing the mass of water absorption (M%) as a function of absorption time (t). The present work represents a new non-destructive evaluation (NDE) technique for detecting the water absorption rate by evaluating the dielectric properties of glass fiber and epoxy resin composite pipes subjected to internal hydrostatic pressure at room temperature. The variation in the dielectric signatures is employed to design an electrical capacitance sensor (ECS) with high sensitivity to detect such defects. ECS consists of twelve electrodes mounted on the outer surface of the pipe. Radius-electrode ratio is defined as the ratio of inner and outer radius of pipe. A finite element (FE) simulation model is developed to measure the capacitance values and node potential distribution of ECS electrodes on the basis of water absorption rate in the pipe material as a function of absorption time. The arrangements for positioning12-electrode sensor parameters such as capacitance, capacitance change and change rate of capacitance are analyzed by ANSYS and MATLAB to plot the mass of water absorption curve against absorption time (t). An analytical model based on a Fickian diffusion model is conducted to predict the saturation level of water absorption (M_S) from the obtained mass of water absorption curve. The FE results are in excellent agreement with the analytical results and experimental results available in the literature, thus, validating the accuracy and reliability of the proposed expert system.

Keywords: electrical capacitance sensor (ECS), composite materials; water absorption rate

1. Introduction

The use of composite materials in structural applications has drastically increased in recent years. The major advantages of composite materials are their unique mechanical properties, in particular the specific strength and specific stiffness, also improved fatigue resistance and damage tolerance capability. It has been due to these properties that composite materials are now extensively used and are becoming the dominant type of material in structural applications, automotive, aerospace, marine and by sports equipment industries. For example, in aircraft structures composites are now widely used in wings, trailing-edge panels and stabilizers. The new

*Corresponding author, Assistant Professor, E-mail: wael.altabey@gmail.com

http://www.techno-press.org/?journal=aas&subpage=7 ISSN: 2287-528X (Print), 2287-5271 (Online)

Boeing B787 has extensively incorporated composite materials in the structure of the aircraft, including the fuselage, which is entirely made of composite materials (Altabey 2015, 2017).

It is highly desirable to have structural health monitoring (SHM) systems in structures for which failures would lead to catastrophic loss of life, i.e., in composite structures. If the onset of failures can be detected, steps can be taken to limit or prevent the use of these structures, while repairs can be made. The SHM aims to determine the health of a structure by data collected from a network of sensors permanently installed on the structure and monitored over time. The goal of a SHM system if first carry out a diagnosis of structural safety and health, followed by the prognosis of the remaining life (Abouelwafa *et al.* 2013, Altabey and Noori 2018).

The difference in non-destructive evaluation (NDE) techniques indicates several difficulties associated with their field application due to their requirements of heat or wave sources and complicated data analysis. Other challenges that NDE methods need to address include, but are not limited to, how to cover large areas for detection, as well as difficulties associated with interpretation of the results.

Currently, ECS is one of the most mature and promising methods, which measures the capacitance change of multi-electrode sensors due to the change of dielectric permittivity being imaged and then reconstructs the cross-section images using the measured raw data with a suitable algorithm. Some of its characteristics and advantages include low cost, fast response, non-intrusive method, broad application and safety (Yang *et al*. 1995a, b, Li and Huang 2000, Mohamad *et al*. 2012 and Zhang *et al*. 2014).

The objective of this study is to present a new practical technique for monitoring of the water absorption rate in composite structures, considering it is one of the most important parameters impacts in the failures of composite structures, especially, aircraft structures by detecting the local variation of the dielectric properties of materials using an electrical capacitance sensor (ECS).

The mechanical properties of polymers and polymer matrix composites can be affected by water absorption (Maggana and Pissis 1999, Peyser and Bascom 1981, Prian and Barkatt 1999). Water can cause plasticization of the polymeric matrix, reducing its fiber-transition temperature (Peyser and Bascom 1981) and cause degradations in strength and mechanical properties (Prian and Barkatt 1999, d'Almeida *et al*. 2008, Zamri *et al*. 2011, Athijayamani *et al*. 2009, Lundgren and Gudmundson 1994, Komai *et al*. 1989, Perreux and Suri 1997). The long-term behavior of composites during their service lives in aggressive environments must, therefore, be analyzed to guarantee a safe operational use of these materials.

It is important to point out that in studying the water absorption detection in composite structures, using ECS technique, there are a few important issues that must be examined before the detection analysis is carried out. These issues have been thoroughly studied in this paper. First, the mechanical properties and attributes of the composite material must be understood. Subsequently, an analytical model based on a Fickian diffusion model is conducted to predict the saturation level of water absorption (MS) from the obtained mass of water absorption curve. Finally, a comparison needs to be made between the results presented in the literature and those obtained in the current study in order to show the advantages of the methodology developed and implemented in this research.

2. Electrical capacitance sensor (ECS)

ECS was first introduced in the 1980s by a group of researchers from the US Department of

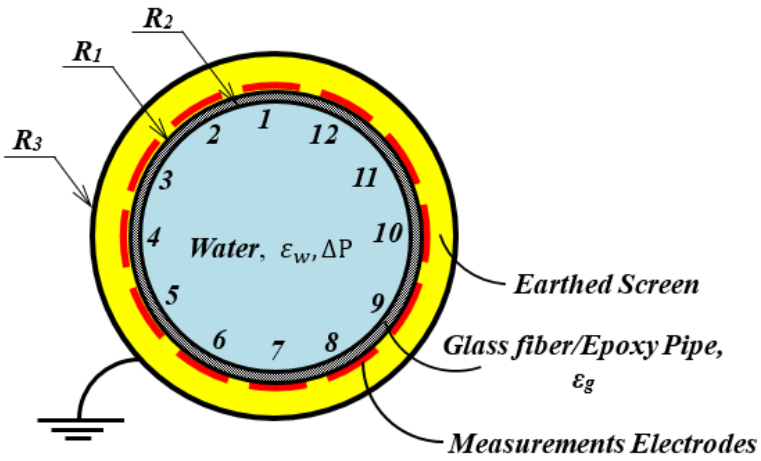

Fig. 1 Cross section sketch of 12-electrode ECS

Energy Morgantown Energy Technology Center (METC), to measure fluidized bed systems (Fasching and Smith 1988, 1991).

An ECS consists of an insulating pipeline, measurement electrodes, radial screen and earthed screen (see Fig. 1). The measurement electrode is mounted symmetrically around the circumference of the insulating pipeline. Radial screen is fitted between the electrodes to cut the electro line external to the sensor pipeline and reduce the inter-electrode capacitance. The earthed screen surrounds the measurement electrodes to shield external electromagnetic noise. ECS converts the permittivity of inner media flow to inter-electrode capacitance, which is the ECS forward problem. Capacitance measuring circuit takes the capacitance data and transfers that to imaging computer. Imaging computer reconstructs the distribution image with a suitable algorithm. This is called ECS inverse problem.

In most applications, ECS electrode is mounted outside the ECS pipeline, which is called external electrode ECS. There are three factors which have large impact on ECS measurements, e.g. pipeline material, inner dielectric permittivity (Jaworski and Bolton 2000, Pei and Wang 2009, Altabey 2010, Asencio *et al*. 2015, Sardeshpande *et al*. 2015, Mohamad *et al*. 2016, Altabey 2016a) and the ratio of the pipeline thickness and diameter (Daoye *et al*. 2009, Altabey 2016b). Later Altabey (2016) found that the ECS environment temperature is effect on ECS sensitivity and sensitive domain of ECS electrodes with high percentage, so the environment temperature is the fourth factor of factors which have influence on ECS measurement sensitivity.

The invention relates to a method for modifying the electric potential change (EPC) for the detection of fatigue cracking and delamination in a basalt fiber reinforced polymer (FRP) laminate composite pipe. Capacitance values, capacitance change and potential distribution of ECS electrode nodes were calculated prior to crack initiation (Altabey and Noori 2017, Zhao *et al*. 2018) and delamination assessment (Altabey 2017a, b). The effect of pipeline environmental temperature on corrosion rates has been further investigated by designing an effective artificial neural network (ANN) architecture (Altabey 2016b).

2.1 The ECS geometric model

The ECS is made up of glass fiber reinforced epoxy composite pipe and has a ring of 12

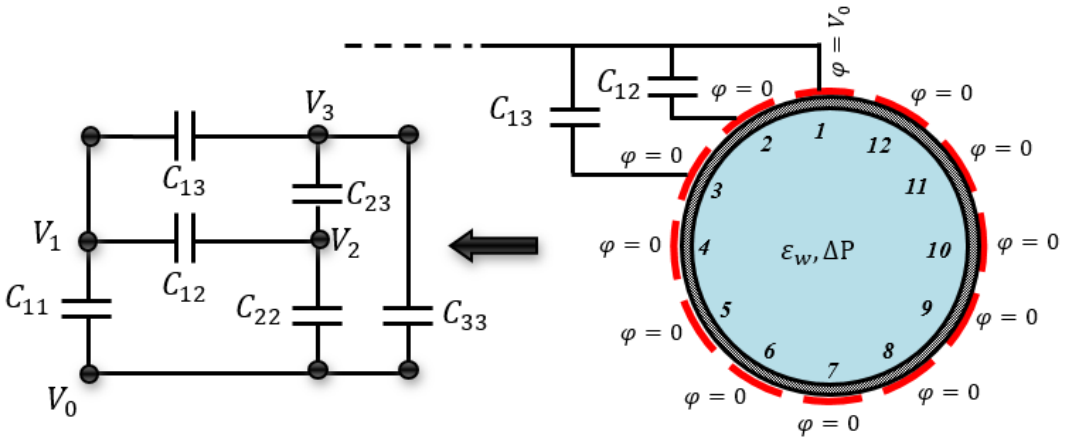

Fig. 2 Schematic representation of the measurement principle of an ECS

electrodes (which are separated from each other by a small gap) on its outer periphery. Fig. 1 is the cross section of 12-electrode ECS system, in which R_1 is the inner composite pipe radius; R_2 is the outer composite pipe radius; R_3 is the earthed screen radius; and radial screen is connected to outer composite pipe. The water is supplied inside the composite pipe from a pump and the model also includes the differential pressure to take into account the pressure difference $(\Delta P = P_1 - P_2)$ of the water, where P_1 is the inlet or high pressure point while P_2 is the outlet or low-pressure point. The dielectric permittivity of glass fiber/epoxy and water are ε_w and ε_g, respectively.

2.2 The ECS composition and working principle

For 12-electrode system, the electrodes are numbered as shown in Fig. 1, are excited with an electric potential, one at a time in increasing order. When one electrode is excited, the other electrodes are kept at ground potential as shown in Fig. 2 and act as detector electrodes. When electrode No. 1 is excited with a potential, the change $Q_{1,j}$ induced on the electrodes, $j = 2, \cdots\cdots, N$, can be measured. Next, electrode No. 2 is excited whereas, rest of the electrodes are kept at ground potential and the induced charges $Q_{23}, Q_{24}, \cdots, Q_{2N}$ $(N = 12)$ are measured. The measurement protocol continues until electrode $N-1$ is excited. Using these charge measurements, the inter electrode capacitance C_{ij} can be computed using the definition of capacitance (Eq. (1)) i.e.,

$$C_{ij} = \frac{Q_{ij}}{\Delta V_{ij}} \tag{1}$$

where Q_{ij} is the charge induced on electrode j when electrode *i* is excited with a known potential. V_{ij} is the potential difference between electrodes *i* and *j* $(\Delta V_{ij} = V_i - V_j)$. So the number of independent capacitance measurements $M = 66$ using Eq. (2) is

$$M = \frac{N(N-1)}{2} \tag{2}$$

Table 1 Physical and mechanical properties of the glass fiber/epoxy.

E_1	$E_2 = E_3$	$G_1 = G_3$	G_2	$\upsilon_1 = \upsilon_3$	υ_2	ρ
53.74 GPa	17.95 GPa	8.63 GPa	5.98 GPa	0.25	0.5	1900 kg/m^3

It is important to note that these capacitances are dependent on the geometry of electrodes and are determined once the size and the location of the electrodes and the permittivity distribution $\varepsilon(x, y)$ are known. A change in the permittivity distribution $\varepsilon(x, y)$ is naturally reflected in the capacitance measurements. The actual capacitance changes measured will be very small, in the order of Pico or Femto Farad (10^{-12}F or 10^{-15}F). Sequential electrodes are referred to as adjacent electrodes; have the largest standing capacitance, while diagonally or opposing electrodes will have the smallest capacitances.

3. Finite element formulations

3.1 Physical properties of the glass fiber/epoxy pipe

Physical and mechanical properties of the glass fiber/epoxy laminate composite pipe are shown in Table 1.

3.2 The geometric properties

The model section comprises of an ECT sensor column with 0.32 m inner diameter and 0.3 m height. Through simulating comparison of full pipe of glass fiber/epoxy and empty pipe, we will get the distribution of electric sensitive potential and media distribution on the sensitive field. The permittivity values of glass fiber/epoxy and air are 3.12 and 1.0 respectively. There are 12 set excitation electrodes and the excitation voltage is 15 volts. The sensors physical specification are shown in Table 2. The remaining electrode and shield grounding simulation status is as follows.

Table 2 Sensor physical specification

ECS system	Specification
No. of electrodes	12
Space between electrodes	2 mm
Pipe diameter (d)	305 mm
Pipe thickness (h)	7.5 mm
Earth Screen diameter	420 mm
Thickness of electrodes	1 mm
Permittivity glass fiber/epoxy	ε_g = 3.12 Fm^{-1}
Permittivity of Water	ε_w = 80 Fm^{-1}
Permittivity of Air	ε_A = 1.0 Fm^{-1}

3.3 ECS governing equation

In terms of Electrical Capacitance sensor (ECS), the forward problem is the problem of calculating the capacitance matrix C from a given set of sensor design parameters and a given cross-sectional permittivity distribution $\varepsilon(x,y)$. The potential distribution $\varphi(x,y)$ inside the ECS is determined by solving the Poisson's equation

$$\nabla.\varepsilon(x,y)\nabla\varphi(x,y) = 0 \tag{3}$$

where $\varphi(x,y)$ is the potential distribution inside the ECS is determined by solving the Poisson's equation. For the boundary condition imposed on the ECS head by the measurement system. The electric field vector $E(x,y)$, the electric flux density $D(x,y)$ and the potential function φ(x,y) are related as follows

$$E(x,y) = -\nabla\varphi(x,y) \tag{4}$$

$$D = \varepsilon(x,y)E(x,y) \tag{5}$$

The change on the electrodes and hence the inter electrode capacitances can be found using the definition of the capacitance and Gauss's law based on the following surface integral

$$Q_{ij} = \oint_{S_j} (\varepsilon(x,y)\nabla\varphi(x,y).\hat{n})\, ds \tag{6}$$

where $\nabla.\varepsilon(x,y)$ is the divergence of permittivity distribution, $\nabla\varphi(x,y)$ is the gradient of potential distribution, S_j is a surface enclosing electrode j, ds is an infinitesimal area on electrode j, $\hat{n}$ is the unit vector normal to S_j and ds is an infinitesimal area on that.

3.4 The FE model description

In this section, the numerical models for simulating the water absorption rate in glass fiber/epoxy pipe will be addressed using ANSYS ver.15. 2D FE software. The approach taken by ANSYS 2D is to divide the different materials and geometries into triangular elements, because many pipes are round under the circumstances of a smaller number of pixels, we can achieve higher accuracy to use the triangular mesh instead of rectangular grids and then to represent the electric field (see Eq. (4)) within each element with a separate polynomial at six integration points location. For FE simulating of glass fiber/epoxy pipe, electrostatic module (PLANE121), triangular 6-node and the element has one degree of freedom, voltage at each node. The 6-node elements have compatible voltage shapes and are well suited to model curved boundaries. The total number of elements used for the analyses was 2322. To improve the accuracy of mesh, we divided the meshed region again into 4518 elements.

3.5 The boundary conditions

The potential boundary conditions were applied to the sensor-plate (electrodes). For one electrode, the boundary condition of electric potential ($V=V_0$) with 15V (V_0) was applied and another electrode was kept at ground (V=0) potential to simulate a 15V (RMS) potential gradient across the electrodes. For representing the natural propagation of electric field, the default boundary condition of continuity $(\hat{n}.(D_1 - D_2) = 0)$ was maintained for the internal boundaries.

4. Results and discussions

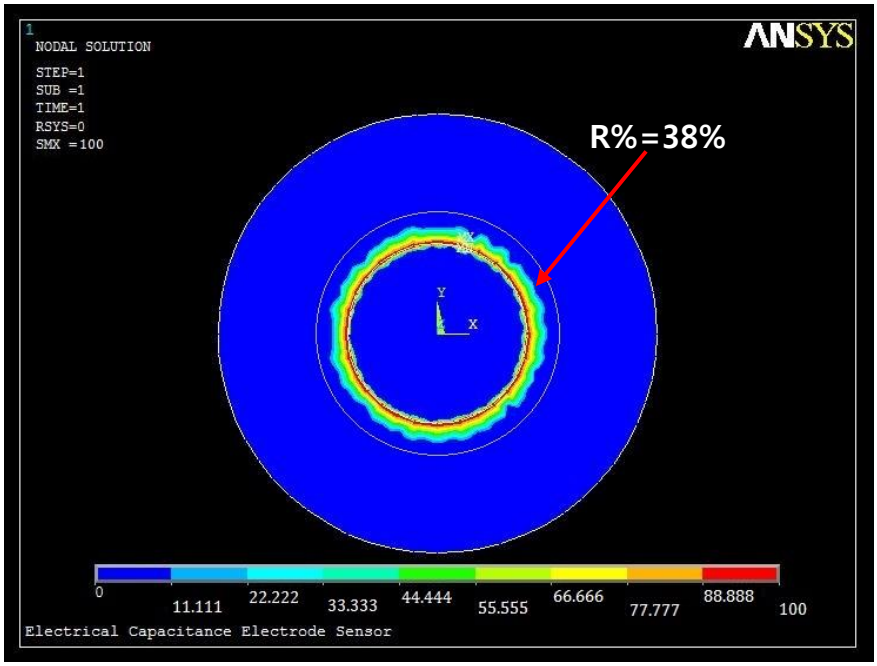

Fig. 3 Water absorption predicted by finite element analysis at 50 days

4.1 Mass of water absorption (M%) detection

The approach taken by a 2D finite element simulation was selected for modeling the sensing system based on forward model proposed by Xie *et al*. 1992. The 2D models considered in this study were constructed using commercially available finite element software, ANSYS (The Electrostatic Module in the Electromagnetic subsection of ANSYS 2015, Al-Tabey 2012, Altabey *et al*. 2018a, b). The software only computes the potential and the electric field values at the element nodes and interpolates between these nodes to obtain the values for other points within the elements. Using the scripting capabilities in ANSYS, simulation in water absorption level plotted by finite element analysis, we can calculate the mass of water absorption ($M\%$) at any absorption time (t) before saturation by Eq. (7)

$$M\% = \frac{E_S - E_F}{E_S} \times 100 \tag{7}$$

where E_S and E_F are the number of elements for saturation and as fabricated cases respectively.

For example, Fig. 3 shows the water absorption predicted by finite element analysis at 50 days, from Fig. 3 and by applying Eq. (7), we can calculate the mass of water absorption was about 0.38 % at 50 days.

The ANSYS 2D simulation model was performed with a fabricated (time of absorption, t = 0) and aged (saturation was reached) GFRE pipe. The absorption times of the aged pipes were selected according to the water absorption characteristics of the composite, with constant working conditions, water pressure ($\Delta P = 11.5$ MPa) and room temperature 25℃. Figs. 4-6 show the effect of water absorption rate (R%) at absorption time variation (t (days)) on node potential distribution of the first electrode for three stages of water absorption rate in a pressurized glass

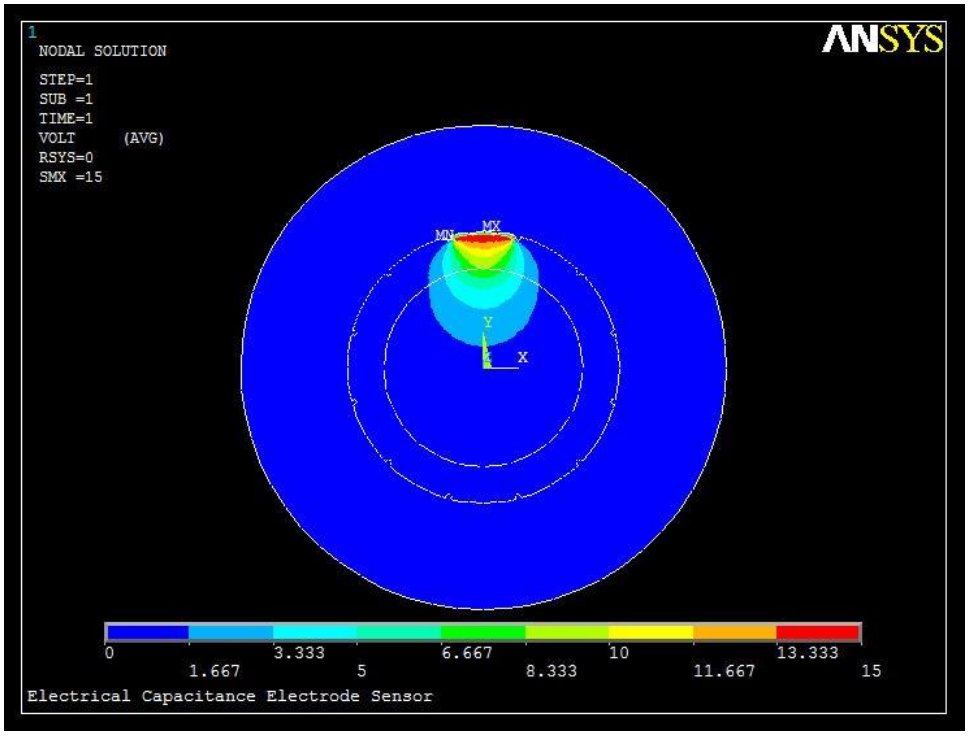

Fig. 4 The node potential distribution of pipe material as fabricated (R% = 0%) at t=0 days

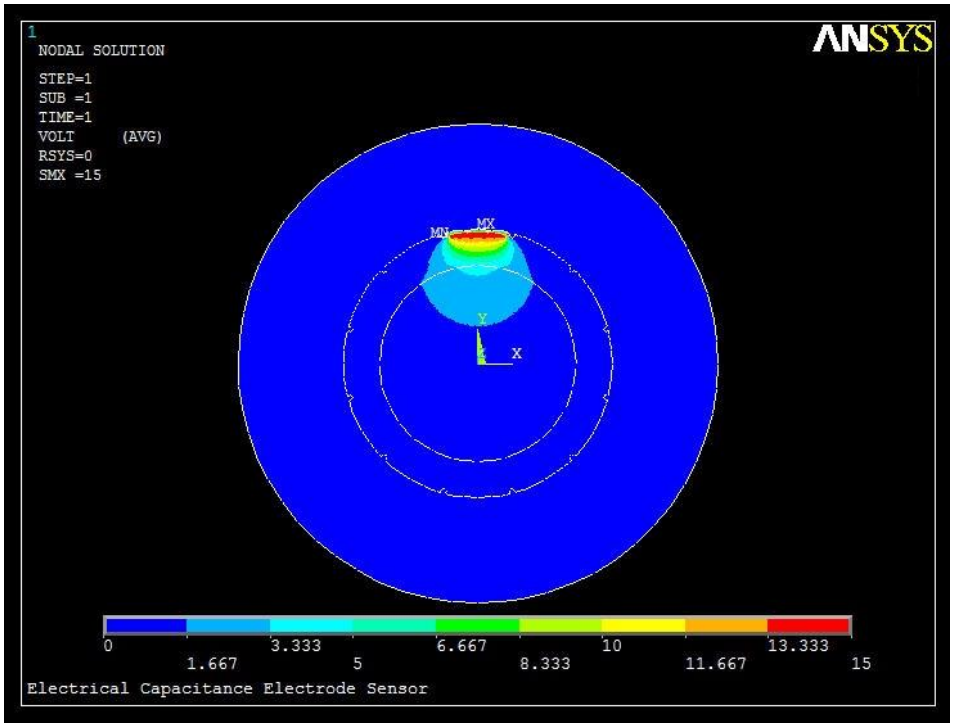

Fig. 5 The node potential distribution of pipe material during absorption (R% = 56.8%) at t=75 days

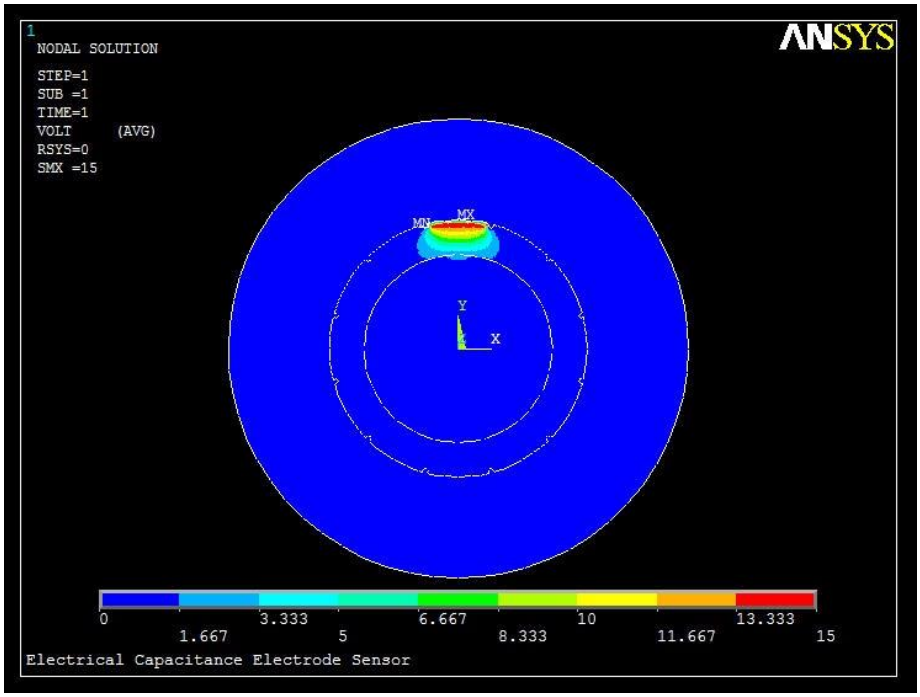

Fig. 6 The node potential distribution of pipe material at saturation stage (R% = 99.6%) at t=245 days

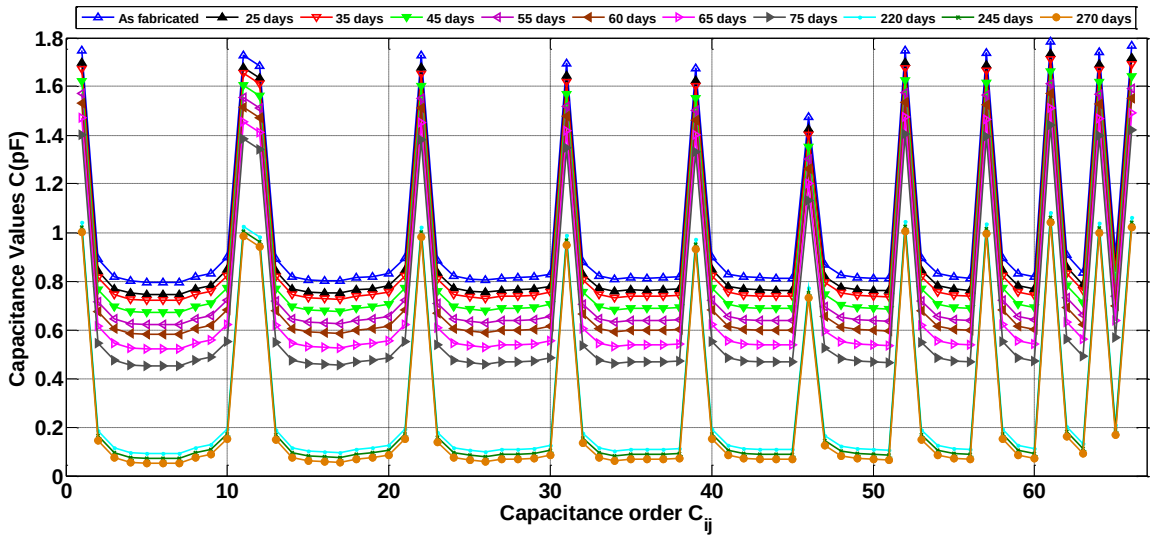

Fig. 7 Simulated capacitances from 2D ANSYS model of glass fiber/epoxy pipe water absorption rate (R%) at different absorption time (t (days))

fiber/epoxy pipe at room temperature, as fabricated (R% = 0%) at t=0 days, during absorption (R% = 56.8%) at t=75 days and saturation stage (R% = 99.6%) at t=245 days, respectively.

The blue area represents the region of the pipe without potential i.e., $\varphi = 0$ but the colored areas represent the region of the pipe that have different potential (different node potential) i.e., the

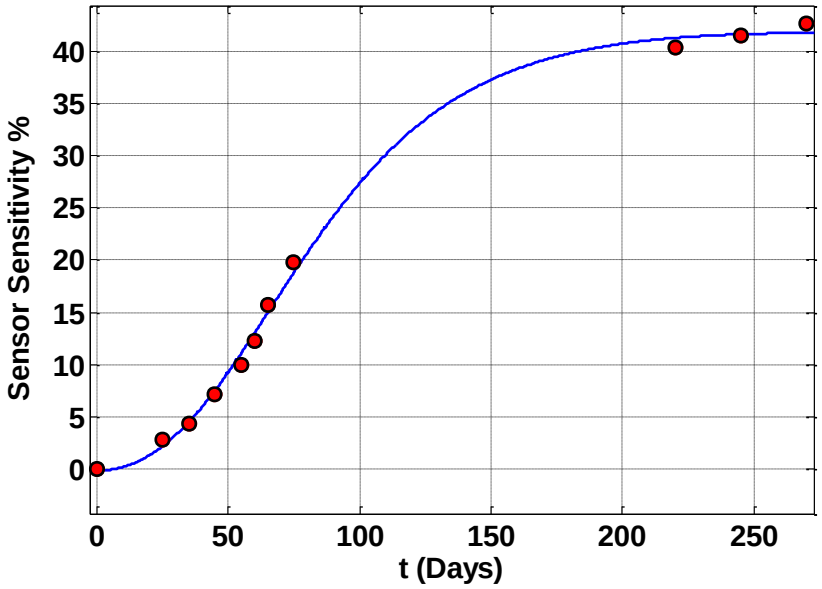

Fig. 8 Capacitance sensor sensitivity versus absorption time (t (days))

domain of electrode can be sensitive or the detection domain.

From the simulation Figs. 4-6, we can make a conclusion that there is a significant difference between the three stages of water absorption rate in the node potential and electric field intensity.

The 66 capacitance measurements (M) of glass fiber/epoxy pipe water absorption at different absorption time (t (days)) from 2D ANSYS model are illustrated in Fig. 7. As shown in the Fig. 7 the absorption times, viz. from 25 days to 75 days, saturation was not yet reached, but saturated pipe material were observed for the longer absorption times.

Fig. 8 shows the sensor sensitivity versus the absorption time (t (days)). The sensor sensitivity is defined as

$$Sensor\ sensitivity\ \% = \frac{C_S - C_F}{C_F} \times 100 \tag{8}$$

where C_S and C_F are the capacitance measurements for saturation and as fabricated cases respectively. The sensor sensitivity increases with the increase in the absorption time, t, as the sensor has a sensitivity ranging between 2.8 and 42.6% for absorption time ranging between 25 and 270 days for selected sensor geometrical parameters.

4.2 Theoretical validation

A Fickian model (Ellyin and Maser 2004) can be used to describe the water absorption data, as shown in Fig. 9. If the initial conditions are uniform and if the geometry allows for the assumption of a unidirectional diffusion through the thickness (thin section, $(h/d) \leq 0.1$), then Fick's law is given by Springer (1981)

$$\frac{M\%}{M_S} = 1 - \frac{8}{\pi^2}\sum_{n=0}^{\infty}\frac{1}{(2n+1)^2}exp\left[-D(2n+1)^2\pi^2\frac{t}{h^2}\right] \tag{9}$$

where $M\%$ is the mass of water absorbed at a time t, M_S is the mass of water absorbed at saturation, h is the pipe thickness and D is the diffusion coefficient.

The diffusion coefficient (D), for the composite specimen was calculated using Eq. (10)

$$D = \pi\left(\frac{kh}{4M_S}\right)^2 \tag{10}$$

where k is the initial gradient of the water absorption curve, as shown in Eq. (11)

$$k = \left(\frac{M_2 - M_1}{\sqrt{t_2} - \sqrt{t_1}}\right)^2 \tag{11}$$

The complete absorption curve can be modeled using the simplified equation represented by McKague *et al*. (1976) for $(\mathrm{M}\%/\mathrm{M_S}) < 0.5$, i.e., for short times in Eq. (9)

$$\frac{M\%}{M_S} = \tanh\left(\frac{4}{h}\sqrt{\frac{Dt}{\pi}}\right) \tag{12}$$

Fig. 9 shows the finite element data of the mass of water absorbed (M%) vs. time (t) curves obtained. The solid curve is the best fit obtained plotting of Eq. (12) using the finite element values.

4.3 Experimental validation

The experimental dataset used in this work is adapted from d'Almeida *et al*. (2008). The tests were conducted on glass fiber composite pipes used for the transport of the so-called service waters. Pipes must maintain their integrity for long periods of time without losing their mechanical performance, although directly exposed to water.

Fig. 9 shows the mass of water absorption (M%) behavior of the GFRE composite pipe and the times of absorption of the pipe material. It can be seen that for the first absorption times, viz. from 25 days to 75 days, saturation was not yet reached, saturation level of water absorption was 0.43% at 270 days water absorption times.

Figs. 9-10 show the comparison between a finite element data of the mass of water absorbed (M%) and experimental data by d'Almeida *et al*. (2008) for the same pipe geometric specifications, initial conditions and absorption times.

From these data we can see the excellent agreement between the finite element and experimental data with an average error of 2.2 %. The deviation between the experimental and finite element data is due to the fact that the 2D finite element simulations ignore the fringe-field effects at the outer edges of the electrodes.

5. Conclusions

A new non-destructive evaluation (NDE) technique based on the change in the dielectric properties of materials was presented. The design methodology of the electrical capacitance sensors (ECS) to detect water absorption rate in the GFRE composite pipes has been developed. The effect of the water absorption rate as a function of the absorption time (t) on the capacitance signals was evaluated using a finite element (FE) simulation model. The FE results clearly show that the difference between the dielectric signatures of GFRE can be used to detect the water

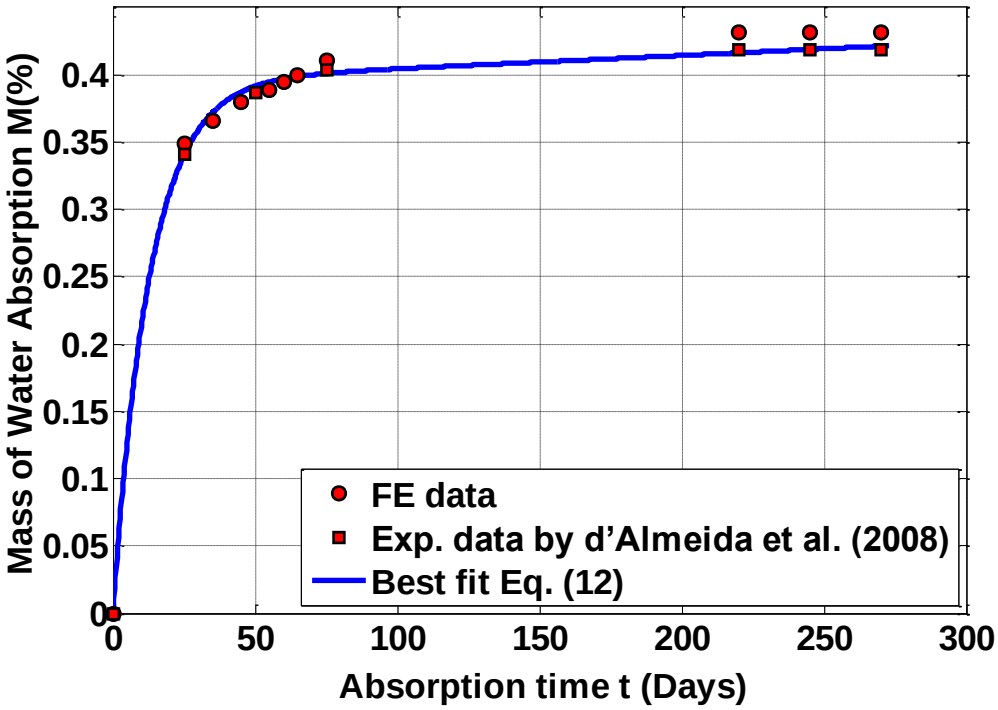

Fig. 9 The mass of water absorption (M%) as a function of absorption time (t (days))

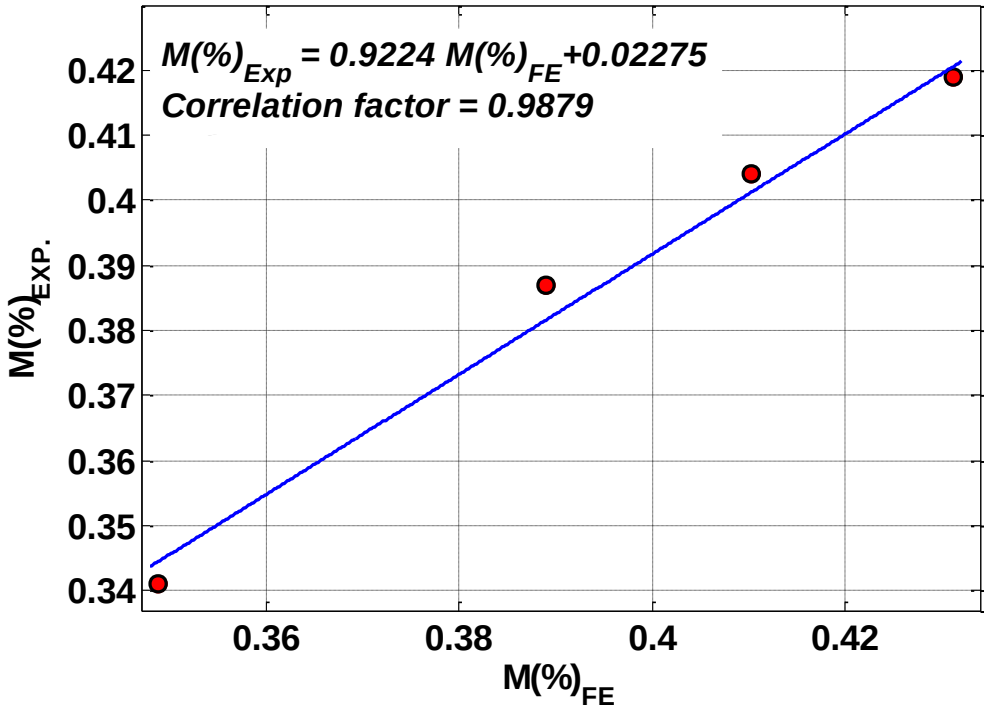

Fig. 10 The experimental and finite element results correlation.

absorption rate in composites and using the scripting capabilities in ANSYS simulation in water absorption level plotting (see Fig. 8) by finite element analysis, we can calculate the mass of water absorption (M%). An analytical model based on a Fickian diffusion model was conducted to predict the saturation level of water absorption (M_S) from the obtained mass of water absorption curve. The simulation results show a sensor sensitivity varied between 2.8 and 42.6% for water absorption time between 25 and 270 days for selected sensor geometrical parameters. The FE model results have been verified using an experimental result available in the literatures. A good agreement was observed with an analytical and an experimental result with an average error of 2.2%, as shown in Figs. 9-10, thus validating the accuracy and the reliability of the proposed expert system.

References

Abouelwafa, M.N., El-Gamal, H.A., Mohamed, Y.S. and Al-Tabey, W.A. (2014), "An expert system for life prediction of woven-roving GFRE closed end thick tube subjected to combined bending moments and internal hydrostatic pressure using artificial neural network", *J. Adv. Mater. Res.*, **845**, 12-17.

Agari, Y., Anan, Y., Nomura, R. and Kawasaki, Y. (2007), "Estimation of the compositional gradient in a PVC/PMMA graded blend prepared by the dissolution-diffusion method", *Polym.*, **48**(4), 1139-1147.

Al-Tabey, W.A. (2012), *Finite Element Analysis in Mechanical Design Using ANSYS: Finite Element Analysis (FEA) Hand Book for Mechanical Engineers with ANSYS Tutorials*, LAP Lambert Academic Publishing, Germany.

Altabey, W.A. and Noori, M. (2017), "An extensive overview of lamb wave technique for detecting fatigue damage in composite structures", *J. Ind. Syst. Eng.*, **2**(1), 1-20.

Altabey, W.A. and Noori, M. (2017), "Detection of fatigue crack in basalt FRP laminate composite pipe using electrical potential change method", *12th International Conference on Damage Assessment of Structures*, *IOP Conf. Series: J. Physics*, **842**(1), 012079, Japan, July.

Altabey, W.A. and Noori, M. (2018), "Fatigue life prediction for carbon fiber/epoxy laminate composites under spectrum loading using two different neural network architectures", *J. Sustain. Mater. Struct. Syst.*, **3**(1), 53-78.

Altabey, W.A. (2010), "Effect of pipeline filling material on electrical capacitance tomography", *Proceedings of the International Postgraduate Conference on Engineering (IPCE 2010)*, Perlis, Malaysia, October 16-17.

Altabey, W.A. (2015), "The fatigue behavior of woven-roving glass fiber reinforced epoxy under combined bending moments and internal hydrostatic pressure", Ph.D. Dissertation, Alexandria University, Egypt.

Altabey, W.A. (2016), "The thermal effect on electrical capacitance sensor for two-phase flow monitoring", *J. Struct. Monitor. Maintenance*, **3**(4), 335-347.

Altabey, W.A. (2016a), "Detecting and predicting the crude oil type inside composite pipes using ECS and ANN", *J. Struct. Monitor. Maintenance*, **3**(4), 377-393.

Altabey, W.A. (2016b), "FE and ANN model of ECS to simulate the pipelines suffer from internal corrosion", *J. Struct. Monitor. Maintenance*, **3**(3), 297-314.

Altabey, W.A. (2017a), "EPC method for delamination assessment of basalt FRP pipe: Electrodes number effect", *J. Struct. Monitor. Maintenance*, **4**(1), 69-84.

Altabey, W.A. (2017b), "Delamination evaluation on basalt FRP composite pipe by electrical potential change", *J. Adv. Aircraft Spacecraft Sci.*, **4**(5), 515-528.

Altabey, W.A., Noori, M. and Wang, L. (2018a), *Using ANSYS for Finite Element Analysis: A Tutorial for Engineers*, *Volume I*, Momentum Press, New York, U.S.A.

Altabey, W.A., Noori, M. and Wang, L. (2018b), *Using ANSYS for Finite Element Analysis: Dynamic*, *Probabilistic*, *Design and Heat*, *Transfer Analysis*, *Volume II*, Momentum Press, New York, U.S.A.

ANSYS, Inc. (2014), *ANSYS Low-Frequency Electromagnetic analysis Guide*, *The Electrostatic Module in*

the Electromagnetic subsection of ANSYS, ANSYS, Inc., U.S.A.
Asencio, K., Bramer-Escamilla, W., Gutiérrez, G. and Sánchez, I. (2015), "Electrical capacitance sensor array to measure density profiles of a vibrated granular bed", *J. Powder Technol.*, **270**, 10-19.
Athijayamani, A., Thiruchitrambalam, M., Natarajan, U. and Pazhanivel, B. (2009), "Effect of moisture absorption on the mechanical properties of randomly oriented natural fibers/polyester hybrid composite", *J. Mater. Sci. Eng. A*, **517**(1-2), 344-353.
d'Almeida, J.R.M., de Almeida, R.C. and de Lima, W.R. (2008), "Effect of water absorption of the mechanical behavior of fiberglass pipes used for offshore service waters", *J. Compos. Struct.*, **83**(2), 221-225.
Daoye, Y., Bin, Z., Chuanlong, X., Guanghua, T. and Shimin, W. (2009), "Effect of pipeline thickness on electrical capacitance tomography", *Proceedings of the 6th International Symposium on Measurement Techniques for Multiphase Flows*, *J. Phys*: *Conference Series*, **147**, 1-13.
Ellyin, F. and Maser, R. (2004), "Environmental effects on the mechanical properties of glass-fiber epoxy composite tubular specimens", *J. Compos. Sci. Technol.*, **64**(12), 1863-1874.
Fasching, G.E. and Smith, N.S. (1988), "High resolution capacitance imaging system", DOE/METC-88/4083; US Dept. Energy, U.S.A.
Fasching, G.E. and Smith, N.S. (1991), "A capacitive system for 3-Dimensional imaging of fluidized-beds", *Rev. Sci. Instr.*, **62**(9), 2243-2251.
Jaworski, A.J. and Bolton, G.T. (2000), "The design of an electrical capacitance tomography sensor for use with media of high dielectric permittivity", *Measurement Sci. Technol.*, **11**(6), 743-757.
Komai, K., Minoshima, K., Shibutai, T. and Nomura, T. (1989), "The influence of water on the mechanical properties and fatigue strength of angle-ply carbon/epoxy composites", *JSME Int. J. Series. 1*, *Solid Mechanics*, *Strength of Materials*, **32**(4), 588-595.
Li, H. and Huang, Z. (2000), *Special Measurement Technology and Application*, Zhejiang University Press, Hangzhou, China.
Lundgren, J.E. and Gudmundson, P. (1994), "Moisture absorption in glass-fibre/epoxy laminates with transverse matrix cracks", *J. Compos. Sci. Technol.*, **59**(13), 1983-1991.
Maggana, C. and Pissis, P. (1999), "Water sorption and diffusion studies in an epoxy resin system", *J. Polym Sci.*, *Part B: Polym Phys.*, **37**(11), 1165-1182.
McKague, Jr. E.L., Reynolds, J.D. and Halkias, J.E. (1976), "Moisture diffusion in fiber reinforced plastics", *J. Eng. Mater. Technol.*, **98**(1), 92-95.
Mohamad, E.J., Rahim, R.A., Leow, P.L., Fazalul, Rahiman, M.H., Marwah, O.M.F., Nor Ayob, N.M., Rahim, H.A. and Mohd Yunus, F.R. (2012), "An introduction of two differential excitation potentials technique in electrical capacitance tomography", *J. Sensors Actuators A*, **180**, 1-10
Mohamad, E.J., Rahim, R.A., Rahiman, M.H.F., Ameran, H.L.M., Muji, S.Z.M. and Marwah, O.M.F. (2016), "Measurement and analysis of water/oil multiphase flow using Electrical Capacitance Tomography sensor", *J. Flow Measurement Instrumentation*, **47**, 62-70.
Pei, T. and Wang, W. (2009), "Simulation analysis of sensitivity for electrical capacitance tomography", *Proceedings of 9th International Conference on Electronic Measurement and Instruments (ICEMI 2009)*, Beijing, China, August.
Perreux, D. and Suri, C. (1997), "A study of a coupling between the phenomena of water absorption and damage in glass/epoxy composite pipe", *J. Compos. Sci. Technol.*, **57**(9-10), 1403-1413.
Peyser, P. and Bascom, W.B. (1981), "The anomalous lowering of the glass transition of an epoxy resin by plasticization with water", *J. Mater Sci.*, **16**(1), 75-82.
Prian, L. and Barkatt, A. (1999), "Degradation mechanism of fiber-reinforced plastics and its implications to prediction of long-term behavior", *J. Mater. Sci.*, **34**(16), 3977-3989.
Sardeshpande, M.V., Harinarayan, S. and Ranade, V.V. (2015), "Void fraction measurement using electrical capacitance tomography and high speed photography", *J. Chem. Eng. Res. Design*, **9**(4), 1-11.
Springer, G.S. (1981), "Environmental effects", *Environmental Effects on Composite Materials*, *Volume 3*, Technomic Pub. Co., Lancaster, United Kingdom.
Xie, C.G., Huang, S.M., Hoyle, B.S., Thorn, R., Lenn, C., Snowden, D. and Beck, M.S. (1992), "Electrical

capacitance tomography for flow imaging: System model for development of image reconstruction algorithms and design of primary sensors", *IEEE Proceedings-G (Circuits*, *Devices and Systems)*, **139**(1), 89-98.

Yang, W.Q., Stott, A.L., Beck, M.S. and Xie, C.G. (1995a), "Development of capacitance tomographic imaging systems for oil pipeline measurements", *Rev*. *Sci*. *Instruments*, **66**(8), 4326.

Yang, W.Q., Beck, M.S. and Byars, M. (1995b), "Electrical capacitance tomography - from design to applications", *Measurement Control*, **28**(9), 261-266

Zamri, M.H., Akil, H.M., Abu Bakar, A., Ishak, Z.A.M. and Wei Cheng, L. (2011), "Effect of water absorption on pultruded jute/glass fiber-reinforced unsaturated polyester hybrid composites", *J*. *Compos*. *Mater*., **46**(1), 51-56.

Zhang, W., Wang, C., Yang, W. and Wang, C. (2014), "Application of electrical capacitance tomography in particulate process measurement - A review", *J*. *Adv*. *Powder Technol*., **25**(1), 174-188.

Zhao, Y., Noori, M., Altabey, W.A. and Wu, Z. (2018), "Fatigue damage identification for composite pipeline systems using electrical capacitance sensors", *J*. *Smart Mater*. *Struct*., doi.org/10.1088/1361-665X/aacc99.

EC